ELSEVIER

Polymer 42 (2001) 10045–10053

polymer

www.elsevier.com/locate/polymer

Photon transmission technique for monitoring swelling of acrylamide gels formed with various crosslinker contents

Önder Pekcan[a,*], Selim Kara[b]

[a]Department of Physics, Faculty of Science and Letters, Istanbul Technical University, Maslak 80626 Istanbul, Turkey
[b]Department of Physics, Trakya University, 22030 Edirne, Turkey

Received in revised form 3 July 2001; accepted 27 July 2001

Abstract

Photon transmission experiments were performed using a UV–visible (UVV) spectrometer during the swelling of polyacrylamide (PAAm) gels. These gels were prepared from acrylamide (AAm) with various *N*,*N*′-methylenebisacrylamide (Bis) contents by free-radical crosslinking copolymerization (FCC) in water and dried before use for swelling experiments. Transmitted light intensity, I_{tr} increased at very early times when PAAm gels are immersed in water, then decreased continuously as swelling time is increased. Decrease in I_{tr} was attributed to the increase in the scattered light intensity, I_{sc} which may originate from the contrast between 'frozen blob clusters' and holes in the swelling gel. Decrease in I_{tr} was modelled using the Li–Tanaka equation from which time constants, τ_1, and collective diffusion coefficients, D_o were determined for various Bis content PAAm gels. τ_1 and D_o were found to be strongly correlated with the wavelength, λ, of I_{tr} and the Bis content of the gel samples. The correlation between λ and τ_1 and D_o predicts the existence of 'frozen blob clusters' in PAAm gels.

Keywords: Polyacrylamide gels; Swelling; Frozen blob clusters

1. Introduction

The structural heterogeneities of a gel affect greatly its physical properties such as its permeability, elasticity and optical properties. It has been shown that the high permeability of polyacrylamide (PAAm) gels is related to the inhomogeneous crosslink distribution [1,2]. The effects of inhomogeneities of the polymer network on the swelling equilibrium of PAAm gels and on the diffusion of water molecules within the gels were examined [3]. The network structure and its inhomogeneities can be varied by changing the concentration of polymers and the proportion of crosslinkers to polymers. A model that relates gel composition with the swelling ratio, turbidity, elastic modulus and volume fraction was described for PAAm gels [4]. The boundary between a transparent state and an opaque, heterogeneous state for a gel as a function of monomer and crosslinker concentrations was determined [5].

Swelling is directly related to the viscoelastic properties of a gel. The gel elasticity and the friction between the network and solvent play an important role in the kinetics of gel swelling [6–8]. It is known that the relaxation time of swelling is proportional to the square of a linear size of the gel [6], a fact that has been confirmed experimentally [8]. One of the most important features of the gel swelling process is that it is isotropic, i.e. when the radius increases to 10%, the axial length increases to 10% in a long cylindrical gel. The elastic and swelling properties of permanent networks can be understood by considering two opposing effects, the osmotic pressure and the restraining force. Usually, the total free energy of a chemically crosslinked network can be separated into two terms; the bulk and the shear energies. The bulk energy of the system is related to the volume change, which is controlled by diffusion. The other important energy, the shear energy, keeps the gel in shape by minimizing the non-isotropic deformation [9,10]. Li and Tanaka [11] have developed a model where the shear modulus, μ, plays an important role that keeps the gel in shape due to the coupling of any changes in different directions. This model predicts that the geometry of the gel is an important factor, and swelling is not just a diffusion process.

Several experimental techniques have been employed to study the kinetics of swelling, shrinking and drying of chemical and physical gels, among which are neutron scattering [12], quasielastic light-scattering [13], macroscopic experiments [14] and in-situ interferometric measurements.

* Corresponding author. Tel.: +90-0212-285-3213; fax: +90-0212-285-6366.
E-mail address: pekcan@itu.edu.tr (Ö. Pekcan).

0032-3861/01/$ - see front matter
PII: S0032-3861(01)00551-1

Using a fluorescence technique, a pyrene (Py) derivative was employed as a fluorescence probe to monitor the polymerization, aging and drying of aluminosilicate gels [15], with peak ratios in emission spectra being monitored during these processes. Steady-state fluorescence (SSF) measurements on the swelling of gels formed by the FCC of methyl methacrylate (MMA) and ethylene glycol dimethacrylate (EGDM) have been reported [16–19]. A Py derivative was used as a fluorescence probe to monitor swelling, desorption and drying in real time during in situ fluorescence experiments. An in situ photon transmission technique for study of the aging of PAAm gels due to multiple swelling was reported from our laboratory [20], where it was observed that the transmitted light intensity, I_{tr} decreases continuously as a PAAm gel is swelled. The decrease in I_{tr} was attributed to the structural inhomogeneities in the gel.

The equilibrium swelling and shrinking processes of PAAm gels in solvent have been extensively studied [21–23]. It has been reported that PAAm gels undergo continuous or discontinuous volume phase transitions with temperature, solvent composition, pH and ionic composition [21]. pH-induced volume transitions of PAAm gels in an acetone/water mixture were studied using a fluorescence technique. When an ionized PAAm gel is allowed to swell in water, extremely interesting patterns appears on the surface of the gel and the volume expansion increases on addition of sodium acrylate [23]. If PAAm gels are swollen in acetone–water mixtures, gel aging time plays an important role during collapse of the network [23]. The kinetics of swelling of PAAm gels were studied by light scattering and the collective diffusion coefficient of the network was measured [6,13]. Small angle X-ray and dynamic light scattering were used to study the swelling properties and mechanical behaviour of PAAm gels [24,25]. It has been known that the swelling and elastic properties of gels are strongly influenced by large scale heterogeneities in the network structure [9,26]. In the swollen state, these imperfections manifest themselves in a nonuniformity of polymer concentration. These large scale concentration heterogeneities do not appear during gelation, but only in the gel swollen to equilibrium [26]. Light scattering experiments by Bastide et al. seem to confirm this picture [27,28].

In this work, in situ photon transmission experiments are reported during the swelling of PAAm gels prepared with various Bis contents. It was observed that I_{tr} at early times increased suddenly and then decreased continuously as the gels are swelled. The decrease in I_{tr} was attributed to the increase in scattered light intensity, I_{sc}, from the gel due to spatial heterogeneities which increase during swelling processes. I_{tr} was measured by a UV–visible (UVV) spectrometric technique and the swelling in PAAm gels was monitored in real time by using the time-drive mode of the UVV spectrometer. The decrease in I_{tr} against time was modelled using the Li–Tanaka equation [11]. Time constants, τ_1, and the collective diffusion coefficients, D_o, were determined for the gel samples of different Bis contents.

2. Kinetics of swelling

Swelling experiments of disc-shaped gels have shown that the relative changes of diameter and thickness are the same, indicating that the gel-swelling processes are not pure diffusional processes. In fact, the equality of the relative changes of diameter and thickness comes from the non-zero shear modulus, μ that results; the change of total shear energy in response to any small change in shape that maintains constant volume element within the gel should be zero. The high friction coefficient, f, between the network and the solvent overdamps the motion of the network, resulting in a diffusion-like relaxation. The equation of the motion of a network element during the swelling can be given by [11]

$$\frac{\partial \vec{u}}{\partial t} = D_o \vec{\nabla}^2 \vec{u} \tag{1}$$

where $\vec{u}$ is the displacement vector measured from the final equilibrium location after the gel is fully swollen ($u = 0$ at $t = \infty$). $D_o = (K + 4\mu/3)/f$ is the collective diffusion coefficient. Here t denotes the time and K the bulk modulus. Eq. (1) has been used with some success to study the swelling of gels [6]. However, the studies did not properly treat the shear deformation that occurs within a gel during swelling, and hence, cannot explain, for example, the isotropic swelling of a cylindrical gel. This shortcoming was due to the shear modulus of the network keeping the system in shape by minimizing the non-isotropic deformation. For a disc-shaped gel, any change in diameter is coupled to a change in thickness. The total energy of a gel can be separated into bulk energy and shear energy. The bulk energy is related to the volume change, which is controlled by diffusion. The shear energy, F_{sh} on the other hand, can be minimized instantly by readjusting the shape of the gel [11].

$$\delta F_{sh} = 0 \tag{2}$$

Each small diffusion process determined by Eq. (1) must couple to a small shear process given by Eq. (2), producing the following relation for a disc-shaped gel

$$\frac{u_r(r,t)}{r} = \frac{u_z(a,t)}{a} \tag{3}$$

where r is the radius and a is the half thickness of the disk gel. Eq. (3) indicates that the relative change in shape of the gel is isotropic, i.e. the swelling rates of a disc in the axial (z) and radial (r) directions are the same.

Simultaneous solution of Eqs. (1) and (2) produces the following equations for the swelling of a gel disc in axial and radial directions [11].

$$u_z(z,t) = u_z(z,\infty) \sum_n B_n e^{-t/\tau_n} \tag{4a}$$

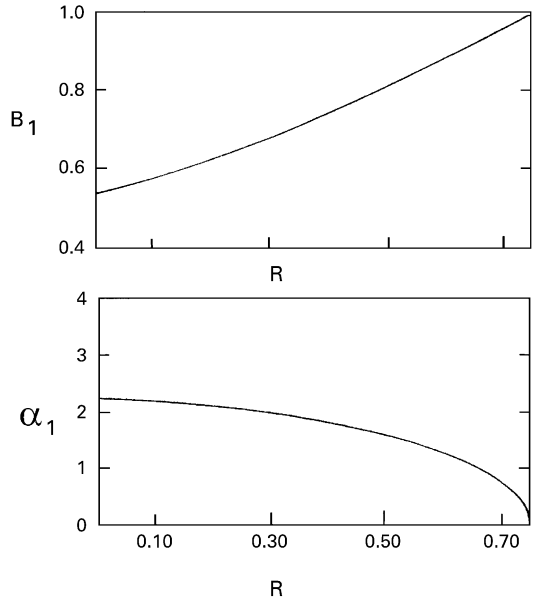

Fig. 1. The relationships B_1–R and α_1–R. Plots are taken from Ref. [11].

$$u_r(r,t) = u_r(r,\infty)\frac{z}{a}\sum_n B_n e^{-t/\tau_n} \tag{4b}$$

where the axial and radial displacements are expressed as series of components, each of them decaying exponentially with a time constant, τ_n. The first terms of the expressions are dominant at large t, that is at the last stage of swelling. Eqs. (4a) and (4b) can also be written in terms of solvent uptakes W and W_∞ at time t and at equilibrium, respectively, as follows

$$\frac{W_\infty - W}{W_\infty} = \sum_{n=1}^{\infty} B_n \exp(-t/\tau_n) \tag{5}$$

In the limit of large t, or if τ_1 is much larger than the rest of τ_n, all higher terms ($n \geq 2$) in Eq. (5) can be omitted and the swelling kinetics is given by the following relation

$$\left(1 - \frac{W}{W_\infty}\right) = B_1 \exp(-t/\tau_1) \tag{6}$$

It should be noted from Eq. (5) that $\sum B_n = 1$, therefore, B_1 should be less than 1. B_1 is related to the ratio of the shear modulus, μ, and longitudinal osmotic modulus, $M = (K + 4\mu/3)$. Hence, once the value of B_1 is obtained, one can determine the value of $R = \mu/M$. Here, we have to note that Eq. (6) can also be obtained by using the theoretical results [11]; in the case of $R \rightarrow 3/4 (\mu/K \rightarrow \infty)$, the time constant $\tau_1 \approx (3/4 - R)^{-1}$ goes to infinity and all the $B_n$tend to zero except B_1 which goes to unity. The dependence of B_1 on R for a disc can be found in the literature [11] (see Fig. 1). τ_1 is related to the collective diffusion coefficient, D_o at the surface of a gel disc by

$$D_o = \frac{3a_\infty^2}{\tau_1 \alpha_1^2} \tag{7}$$

where α_1 is a function of R only and is given in the literature [11] (see Fig. 1), and a_∞ stands for the half thickness of the gel in the final equilibrium state. Hence, D_o can be calculated.

3. Turbidity of gels and frozen blobs

It is well known that scattering causes turbidity when a light beam is passed through a solution. Light scattering is caused by density and concentration fluctuations, i.e. by deviations of density and concentration from their uniform values in a dispersed medium. Light is scattered only when the light wavelength, λ, is greater than the size of a particle of the dispersed phase. If λ is much smaller than the particle diameter, light is reflected. The intensity of incident light is I_o and on passage of the light through a dispersed medium, the incident intensity is reduced to I_{sc} as a result of scattering. Rayleigh derived an equation by excluding the absorption of light by the medium, which connects I_o with I_{sc}. The intensity of light scattered per unit volume of a dilute system is as follows [29].

$$I_{sc} = I_o k c v^2 \lambda^{-\eta} \tag{8}$$

This equation is valid for spherical particles that do not conduct electric current and are small in comparison with, λ. In Eq. (8), k is given by

$$k = 24\pi^3\left(\frac{n_1^2 - n_o^2}{n_1^2 + 2n_o^2}\right) \tag{9}$$

where n_1 and n_o are the refractive indices of the dispersed phase and the dispersion medium, respectively. In Eq. (8), v is the volume of a single particle and c is the concentration of particles, i.e. the number of particles in 1 cm^3 of the system. Rayleigh's equation predicts the turbidity of the medium and can be used for particles whose sizes are not more than 0.1λ, i.e. for particles of diameters from 40 to 70 nm. In this case, I_{sc} changes in inverse proportion to the fourth power of λ ($\eta = 4$ in Eq. (8)). However, for larger particles I_{sc} changes in inverse proportion to smaller powers of λ. The dependence of η on particle size was studied in monodispersed latex systems of polystyrene [29] and it was observed that η decreased from 4 to 2.8.

When the size of particles in the dispersed medium becomes much greater than λ, light is not more scattered but reflected, regardless of the wavelength of the incident light. If the particles are too large in size, reflection of light from them increases which causes the reduction of the intensity of scattered light. In conclusion, Rayleigh's equation shows that for particles of a given size, the intensity of scattered light is directly proportional to the concentration of particles. This relationship can be used to determine the concentration of a dispersed phase by measuring I_{sc} in a system. However, since multiple scattering occurs at very high concentrations, precautions have to be taken. At a given concentration and particle size, the variation of λ

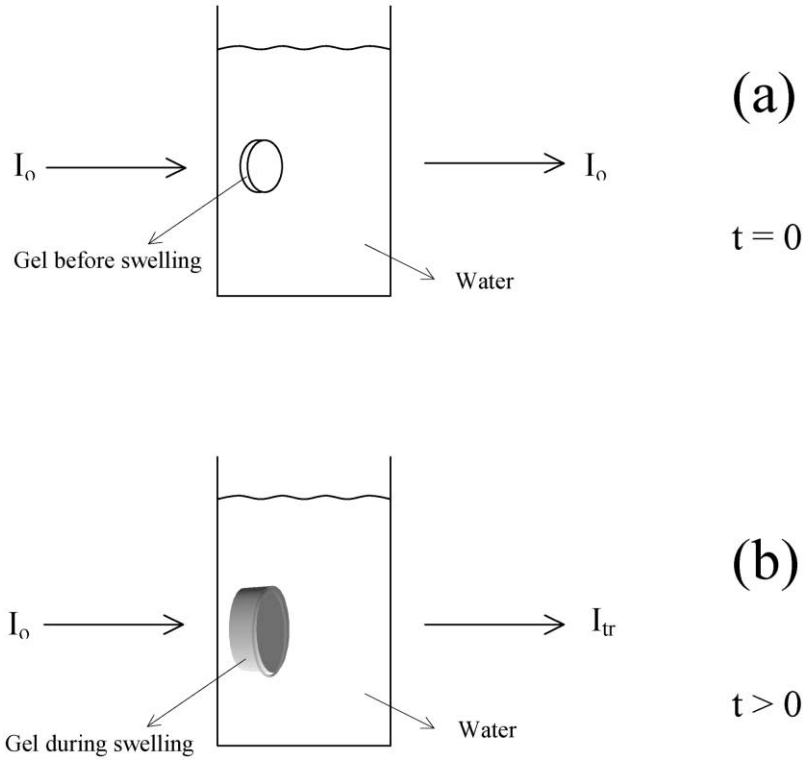

Fig. 2. Representation of a gel (a) before and (b) during the swelling process.

with I_{sc} can enable determination of the exponent η, allowing determination of the particle size.

A gel can be described as a random distribution of crosslinks on a lattice formed by the interchain contact points. When two junctions are located on neighbouring lattice sites, a 'frozen blob' is formed in that region [28]. In the swollen state of a gel, these crosslinks cannot move apart from each other, because they are chemically connected by a chain segment. This segment is in an optimal chain conformation. Frozen blobs are often connected and form clusters of first topological neighbours. As a result, the random crosslinking of chains can be described as a site percolation on a blob lattice. When a gel is in a good solvent, it swells and frozen blob clusters expand less than the interstitial medium.

When a gel is in a swollen state, small clusters are expelled from larger ones, creating regions of low concentration. Here, the correlation length becomes the typical size of holes that are created as a part of the interstitial medium. The swelling of a gel leads to an excess scattering of light that comes from the contrast between frozen blob clusters and holes. During the swelling, the partial separation of frozen blob clusters leads to a strong increase in the scattering intensity, I_{sc} or decrease in the transmitted light intensity, I_{tr}.

4. Experimental

Each gel was prepared by using 2.5 g of AAm and 40 mg of ammonium persulfate (APS) as an initiator by dissolving them in 25 cm^3 of water in which 10 μl of tetramethyl ethylenediamine were added as an accelerator. Seven different gels were obtained by adding 100, 125, 150, 175, 200, 250 and 300 mg Bis into the preceding mixture. Gelation experiments were performed at room temperature in a cylindrical cell of 1.6 cm diameter. Disc-shaped gels were obtained by cutting the cylindrical gels. For the UVV experiments 1.4–1.6 mm thick gels at various Bis contents were placed in a 1 cm × 1 cm quartz cell filled with water. The swelling of the gels was monitored in real time and in situ photon transmission measurements were performed using a Perkin–Elmer UVV spectrometer. A gel before and after swelling is started is presented in Fig. 2a and b, respectively. Photon transmission intensities, I_{tr}, during swelling of gels were measured at five different wavelengths (440, 500, 550, 600, 690 nm) by using the time-drive mode of the spectrometer. Typical normalized I_{tr} curves against swelling time, t_s, are given in Fig. 3 for the experiments made at 500 nm wavelength for seven different Bis content samples. In Fig. 4, I_{tr} curves at various wavelengths are compared for the 250 mg Bis content sample. In Fig. 3, it is seen that I_{tr} increases rapidly at early times, reaching a maximum transparency. Then, except for the 100 and 125 mg Bis content samples, I_{tr} decreases continuously showing the creation of turbidity in these gel samples due to contrast between frozen blobs and holes. The early time behaviour of I_{tr} can be related to the initial stage of diffusion of solvent into the gel. Further swelling shows that the 150,

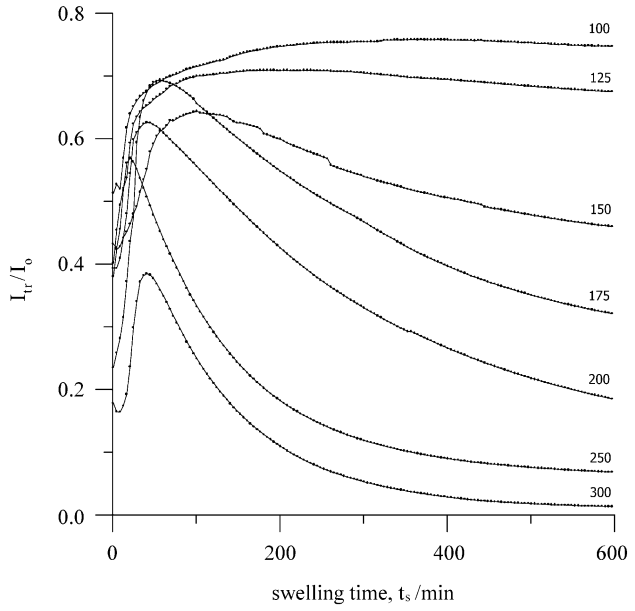

Fig. 3. Variation in normalized transmitted photon intensities, I_{tr}/I_o versus swelling time, t_s, during the swelling process for different Bis content samples at 500 nm wavelength. Numbers on each curve present the Bis content in mg.

175, 200, 250 and 300 mg Bis content gels present lattice heterogeneities that increase due to the swelling process. However, gels with 100 and 125 mg Bis contents show perfect, homogeneous lattice structures during the swelling process, with I_{tr} continuing to increase and saturate at longer times. The different behaviour of I_{tr} in Fig. 4 at various

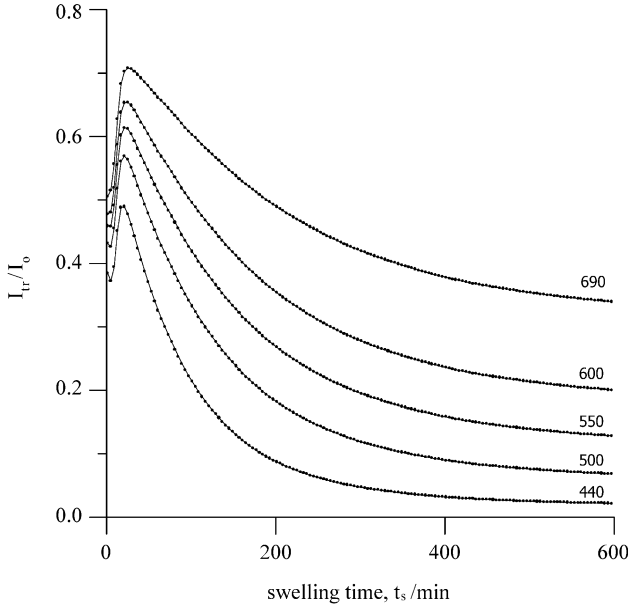

Fig. 4. Variation in normalized transmitted photon intensities, I_{tr}/I_o versus swelling time, t_s, for the 250 mg Bis content sample at various wavelengths. The number on each curve indicates the wavelength of the transmitted light intensity in nm.

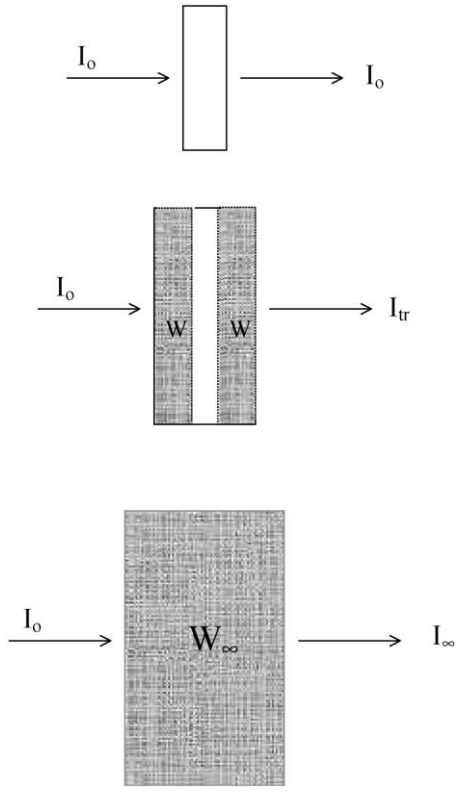

Fig. 5. Representation of solvent uptake during the swelling process and its relation with transmitted light intensity, I_{tr}.

wavelengths may be caused by different sizes of frozen blob clusters, because light scattering is strongly correlated with the wavelength of the light and the size of the scattered centre.

5. Results and discussion

The behaviour of I_{tr} after the maxima can be quantified by establishing the relation between Eq. (6) and I_{tr}. At the maxima, before solvent penetration starts, the transmitted intensity is I_o. After solvent penetration starts, due to the turbidity created by frozen blob clusters, the transmitted intensity decreases to I_{tr} at the swelling time t_s when the amount of solvent uptake is W. At the equilibrium state of swelling, the transmitted intensity decreases to I_∞, and the solvent uptake is W_∞. The relation between solvent uptake, W, and transmitted intensities from the gel during the swelling process is given by the following relation

$$\frac{W}{W_\infty} = \frac{I_o - I_{tr}}{I_o - I_\infty} \tag{10}$$

The swelling process is presented in Fig. 5. Since $I_o \gg I_\infty$, Eq. (10) becomes

$$\frac{W}{W_\infty} = 1 - \frac{I_{tr}}{I_o} \tag{11}$$

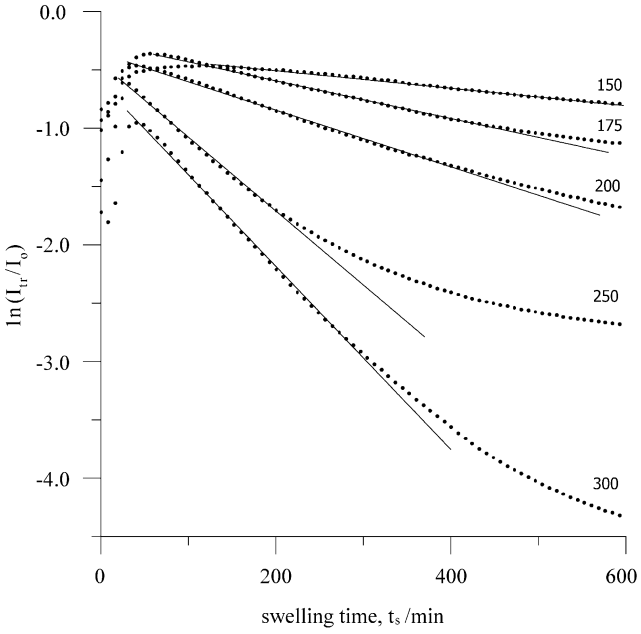

Fig. 6. Plot of the results in Fig. 3 according to Eq. (12). The number on each curve represents the Bis content in mg.

This relation predicts that as W increases, I_{tr} decreases. Combining Eq. (11) with Eq. (6) and taking logarithms, the following relation can be obtained

$$\ln(I_{tr}/I_o) = \ln B_1 - \frac{t_s}{\tau_1} \tag{12}$$

where $t = t_s$ is taken in Eq. (6) to present the swelling time in Eq. (12).

The data in Fig. 3 are plotted in Fig. 6 according to Eq. (12) and the linear portions are used for analysis. Linear regression of this part of data in Fig. 6 provide us with B_1 and τ_1 values, i.e. intercepts and slopes of the straight lines in Fig. 6 produce B_1 and τ_1 values, respectively. Taking into account the dependence of B_1 and R, one obtains R values, and from the $\alpha_1 - R$ dependence, α_1 values were obtained (see Fig. 1). Then, using Eq. (7), collective diffusion coefficients D_o were determined. Similar calculations were made for the UVV experiments at other wavelengths and the results are listed in Table 1 together with the a_i, a_∞ and W_∞ values. Here, a_i and a_∞ are the half-thicknesses of the gels before and after swelling. W_∞ is the solvent uptake at equilibrium swelling. The measured time constants, τ_1, and collective diffusion coefficients are plotted versus Bis content in Fig. 7a and b, respectively. It is seen in Fig. 7a that τ_1 values exponentially decrease as the Bis content is increased, indicating that the swelling of loosely formed gels takes longer than that of densely formed gels. As a result, D_o values are smaller in loosely formed gels than densely formed gels. This behaviour can be understood by realizing the fact that loosely formed gels are more flexible and the shear energy is much less in these gels than in densely formed gels. As the crosslinker density of the gels

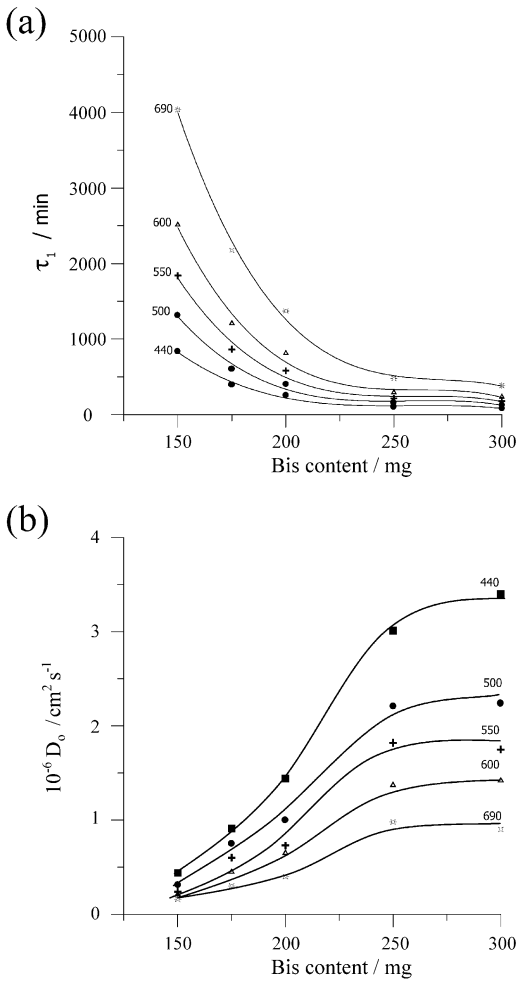

Fig. 7. Plots of (a) τ_1 and (b) D_o versus Bis content. The number on each curve indicates the wavelength of the light.

increases, the shear energy increases. As a result, D_o values increase, i.e. gel segments move faster in densely formed gels than loosely formed gels.

It should be noticed that in Fig. 7 both τ_1 and D_o values change with λ, showing that various sizes of frozen blob clusters are detected by different wavelengths. If one assumes that the size of a 'frozen blob cluster' is proportional to λ, then there should be same relation between τ_1 and λ. In Fig. 8a, τ_1 is plotted versus λ for the 150 mg Bis-content sample. It is seen that τ_1 increases as λ is increased. This behaviour of τ_1 indicates that large frozen blob clusters expand much slower than smaller ones in a loosely formed gel. A similar plot for D_o is shown in Fig. 8b. D_o values decrease as λ is increased for the 300 mg Bis-content sample. In other words, water molecules move faster in small frozen blob cluster than in large ones in the densely formed gel. The λ dependencies of τ_1 and D_o predict the existence of the size distribution of 'frozen blob clusters' for a given gel with a certain Bis content; in fact, the curves in Fig. 8a and b characterise the size distribution of 'frozen blob clusters' in a given gel sample.

Table 1
Experimentally obtained parameters B_1 and τ_1 from the intercepts and the slopes of the straight lines in Fig. 6. D_o was obtained using Eq. (7). W_∞, a_∞ and a_i were measured using a microbalance and callipers

Bis (mg)	100	125	150	175	200	250	300
440 nm							
B_1	0.741	0.688	0.649	0.722	0.652	0.576	0.480
τ_1 (min)	–	–	839	392	258	105	85
D_o ($\times 10^{-8}$ cm^2/s)	–	–	44	91	144	301	340
W_∞ (g)	0.44	0.45	0.42	0.46	0.43	0.44	0.42
a_∞ (mm)	1.6	1.6	1.75	1.6	1.75	1.75	1.75
a_i (mm)	0.75	0.70	0.75	0.70	0.75	0.80	0.80
500 nm							
B_1	0.782	0.733	0.702	0.769	0.705	0.642	0.534
τ_1 (min)	–	–	1319	604	401	157	129
D_o ($\times 10^{-8}$ cm^2/s)	–	–	31	75	100	221	224
W_∞ (g)	0.44	0.45	0.42	0.46	0.43	0.44	0.42
a_∞ (mm)	1.6	1.6	1.75	1.6	1.75	1.75	1.75
a_I (mm)	0.75	0.70	0.75	0.70	0.75	0.80	0.80
550 nm							
B_1	0.804	0.761	0.732	0.789	0.727	0.677	0.565
τ_1 (min)	–	–	1838	864	583	214	177
D_o ($\times 10^{-8}$ cm^2/s)	–	–	24	60	73	182	175
W_∞ (g)	0.44	0.45	0.42	0.46	0.43	0.44	0.42
a_∞ (mm)	1.6	1.6	1.75	1.6	1.75	1.75	1.75
a_i (mm)	0.75	0.70	0.75	0.70	0.75	0.80	0.80
600 nm							
B_1	0.819	0.788	0.757	0.810	0.756	0.702	0.598
τ_1 (min)	–	–	2514	1209	813	293	237
D_o ($\times 10^{-8}$ cm^2/s)	–	–	21	45	65	137	142
W_∞ (g)	0.44	0.45	0.42	0.46	0.43	0.44	0.42
a_∞ (mm)	1.6	1.6	1.75	1.6	1.75	1.75	1.75
a_i (mm)	0.75	0.70	0.75	0.70	0.75	0.80	0.80
690 nm							
B_1	0.852	0.832	0.797	0.843	0.798	0.746	0.638
τ_1 (min)	–	–	4034	2173	1371	478	385
D_o ($\times 10^{-8}$ cm^2/s)	–	–	16	30	40	98	90
W_∞ (g)	0.44	0.45	0.42	0.46	0.43	0.44	0.42
a_∞ (mm)	1.6	1.6	1.75	1.6	1.75	1.75	1.75
a_i (mm)	0.75	0.70	0.75	0.70	0.75	0.80	0.80

Values of I_{tr}/I_o for a given time from Fig. 4 are converted to the scattering light intensity, I_{sc}, and fitted to Eq. (8). Fig. 9 presents log I_{sc} versus log λ for the 250 mg Bis-content sample at a swelling time of 3 h. The slope of this plot produces the value of η. Similar plots are obtained at other swelling times and for various Bis content samples. The derived η values for all gel samples versus swelling time, t_s are plotted in Fig. 10. It is seen that η values increase and saturate for the 150 mg Bis-content sample. However, for the 250 and 300 mg Bis-content samples, η values started to decrease immediately after reaching maxima. For the 175 and 200 mg Bis-content samples, η values reach maximum values and then decrease slightly. As indicated previously, η values are strongly dependent on the particle size that scatters the light. If η is smaller than 2.8, the diameters of particles must be much larger than 70 nm [29]. Here, one can argue that during swelling the sizes of frozen blob clusters increase, i.e. η values increase, causing strong scattering from the swollen gel. The curves in Fig. 10 predict that the sizes of frozen blob clusters are much larger in 250 and 300 mg Bis-content gels than in the other ones. The low crosslinker contents in the 100 and 125 mg Bis-content gels are not sufficient to form large frozen blob clusters. However, the higher crosslinker densities in the 250 and 300 mg Bis-content gels are sufficient to form large frozen blob clusters. Gel samples with 175 and 200 mg Bis contents form frozen blob clusters of medium size (most probably around 100 nm).

The most important conclusions in this paper are presented in Fig. 8a and b where τ_1 and D_o show strong correlations with wavelength, λ. It is believed that these correlations give strong evidence to the existence of 'frozen blob clusters' in acrylamide gels, a significant finding supporting the heterogeneous crosslinking in these

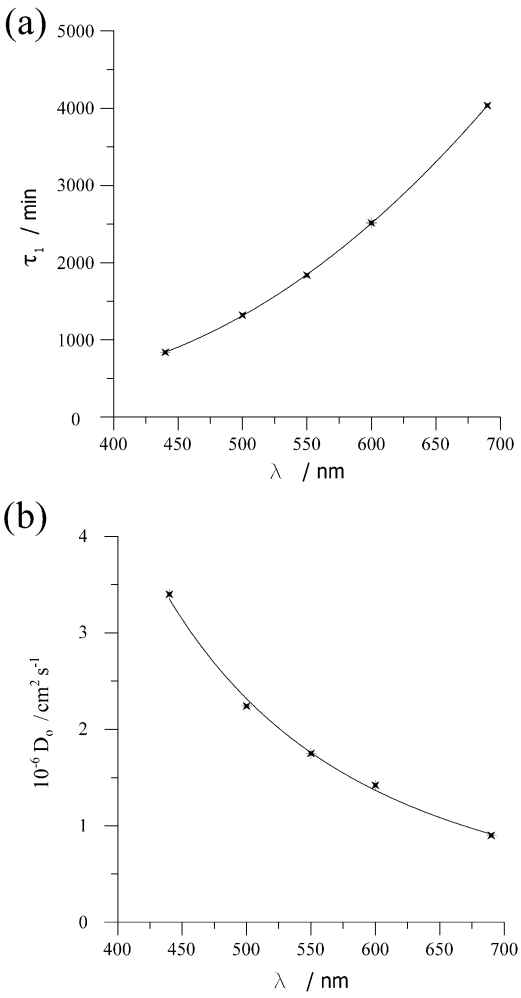

Fig. 8. Plots of (a) τ_1 versus λ for 150 mg and (b) D_o versus λ for 300 mg Bis-content samples.

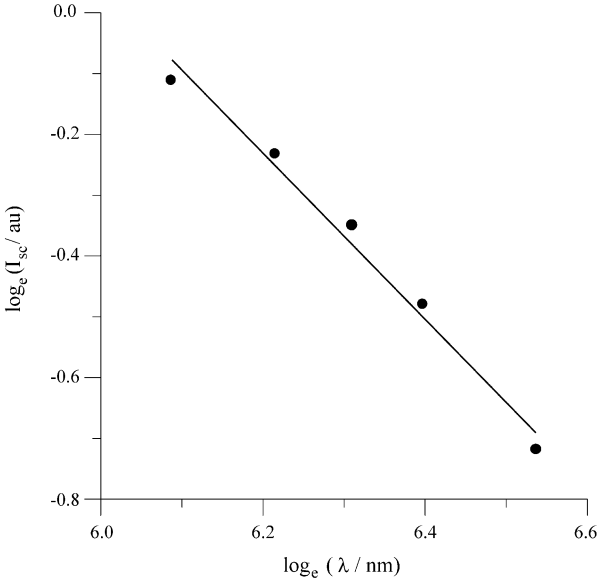

Fig. 9. Log I_{sc} versus log λ for the 250 mg Bis-content sample at a swelling time of 3 h. The slope of the curve produces the value of η plotted in Fig. 10.

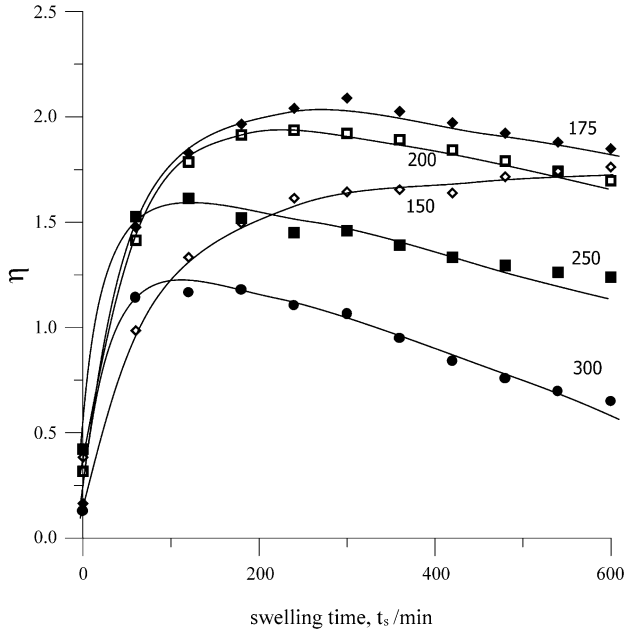

Fig. 10. Plot of η versus swelling time for the gel samples at various Bis-contents. The number on each curve presents the Bis-content in mg.

gels. The λ dependencies of τ_1 and D_o do not present macroscopic behaviour, because they originate from 'frozen blob clusters' representative of the microscopic heterogeneous structures of the gels.

References

[1] Weiss N, Silberger A. Polym Prepr (Am Chem Soc Div Polym Chem) 1975;16(2):289.
[2] Weiss N, van Vliet T, Silberger A. J Polym Sci Polym Phys Ed 1974;17:2229.
[3] Hsu TP, Ma DS, Cohen C. Polymer 1983;24:1273.
[4] Richards EG, Temple JC. Nat Phys Sci 1971;230:92.
[5] Suzuki Y, Nozaki K, Yamamoto T, Itoh K, Nishio I. J Chem Phys 1992;97:3808.
[6] Tanaka T, Filmore D. J Chem Phys 1979;70:1214.
[7] Peters A, Candau SJ. Macromolecules 1986;19:1952.
[8] Chiarelli P, De Rossi D. Progr Colloid Polym Sci 1988;78:4.
[9] Dusek K, Prins W. Adv Polym Sci 1969;6:1.
[10] Candau SJ, Bastide J, Delsanti M. Adv Polym Sci 1982;7:44.
[11] Li Y, Tanaka T. J Chem Phys 1990;92(2):1365.
[12] Bastide J, Duoplessix R, Picot C, Candau SJ. Macromolecules 1984;17:83.
[13] Peters A, Candau SJ. Macromolecules 1988;21:2278.
[14] Wu C, Yang CY. Macromolecules 1994;27:4516.
[15] Panxviel JC, Dunn B, Zink JJ. J Phys Chem 1989;93:2134.
[16] Pekcan Ö, Yilmaz Y. J Appl Polym Sci 1997;63:1777.
[17] Pekcan Ö, Yilmaz Y, Uğur Ş. Polym Int 1997;44:447.
[18] Yilmaz Y, Pekcan Ö. Polymer 1998;39:5351.
[19] Pekcan Ö, Yılmaz Y. In: Rettig W, Strehnnel B, Schrader S, editors. Applied fluorescence in chemistry, biology and medicine, Vol. 331. Berlin: Springer, 1999.
[20] Pekcan Ö, Çatalgil-Giz H, Çalıskan M. Polymer 1998;39:4453.
[21] Hirokawa Y, Tanaka T. J Chem Phys 1984;81:6379.
[22] Hu Y, Horie K, Ushiki H. Macromolecules 1992;25:6040.

[23] Tanaka T, Sun ST, Hirokawa Y, Katayama S, Kucera J, Hirose Y, Amiya T. Nature 1987;325:796.
[24] Ilavsky M. Macromolecules 1982;15:782.
[25] Patel SK, Rodriguez F, Cohen C. Polymer 1989;30:2198.
[26] Silberberg A. In: Kramer O, editor. Biological and synthetic networks. Amsterdam: Elsevier, 1988.
[27] Bastide J, Leibler L. Macromolecules 1988;21:2649.
[28] Bastide J, Bove F, Busier M. In: Baumgartner A, Picot C, editors. Molecular basis of polymer networks. Berlin: Springer, 1989. p. 48.
[29] Voyutsky S. Colloid chemistry. Moscow: Mir, 1978.